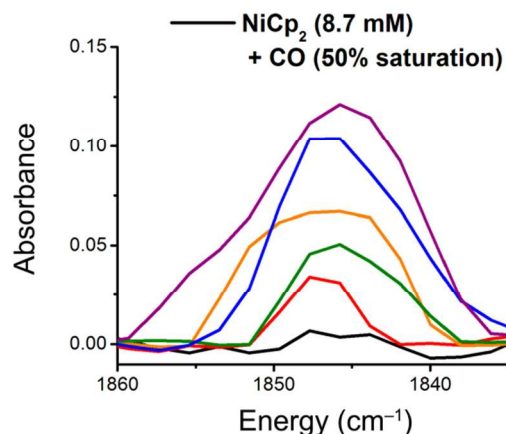


**Developing a Mechanistic Understanding of Molecular Electrocatalysts for CO<sub>2</sub>  
Reduction Using Infrared Spectroelectrochemistry**

Charles W. Machan, Matthew D. Sampson, Steven A. Chabolla, Tram Dang,  
Clifford P. Kubiak\* (\* - [ckubiak@ucsd.edu](mailto:ckubiak@ucsd.edu))

University of California, San Diego  
Department of Chemistry & Biochemistry  
9500 Gilman Drive  
La Jolla, CA 92093-0358

*Supporting Information*



**Figure S1.** Growth of absorbance consistent with the formation of  $[\text{Ni}(\mu_1\text{-CO})\text{Cp}]_2$  dimer (**16**) at  $1845\text{ cm}^{-1}$  under partially saturated CO atmosphere. Reflectance FTIR-SEC spectra obtained sequentially in  $0.1\text{ M TBAPF}_6/\text{MeCN}$  (50% CO saturation) at  $-2.00\text{ V}$  (vs  $\text{Ag}/\text{Ag}^+$ ). Conditions:  $\text{NiCp}_2$  (**14**,  $8.7\text{ mM}$ ) with a glassy carbon WE, Pt CE, and Ag pseudo-RE.

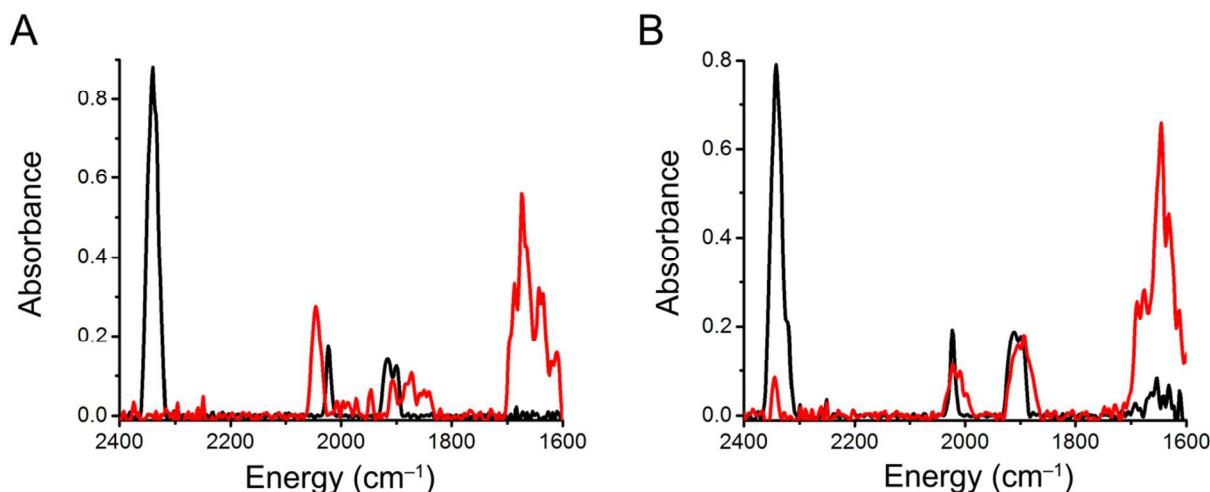


**Figure S2.** Resting potential (black) and final catalytic (red) reflectance IR-SEC spectra of  $\text{Re}^{\text{I}}(\text{dmb})(\text{CO})_3\text{Cl}$  (**1B**) in the presence (**A**) and absence (**B**) of  $\text{Ni}^{\text{II}}\text{Cp}_2$  (**14**). Growth of absorbances consistent with the formation of  $[\text{Ni}^{\text{I}}(\mu_1\text{-CO})\text{Cp}]_2$  dimer (**16**) at  $1845\text{ cm}^{-1}$  and  $\text{Ni}^{\text{I}}(\text{CO})_4$  (**17**) at  $2045\text{ cm}^{-1}$  observed for **A** and not **B**. Additional, unassigned features overlapping with Re carbonyl species are also observed. Reflectance IR-SEC spectra obtained in  $0.1\text{ M TBAPF}_6/\text{MeCN}$  (50%  $\text{CO}_2$  saturation,  $\sim 0.14\text{ M}$ ) at resting potential and  $-2.00\text{ V}$  (vs  $\text{Ag}/\text{Ag}^+$ ), respectively. **A**:  $\text{Re}^{\text{I}}(\text{dmb})(\text{CO})_3\text{Cl}$  (**1B**,  $2.5\text{ mM}$ ),  $\text{Ni}^{\text{II}}\text{Cp}_2$  (**14**,  $7.8\text{ mM}$ ). **B**:  $\text{Re}^{\text{I}}(\text{dmb})(\text{CO})_3\text{Cl}$  (**1B**,  $3.5\text{ mM}$ ). Glassy carbon WE, Pt CE, and Ag pseudo-RE.

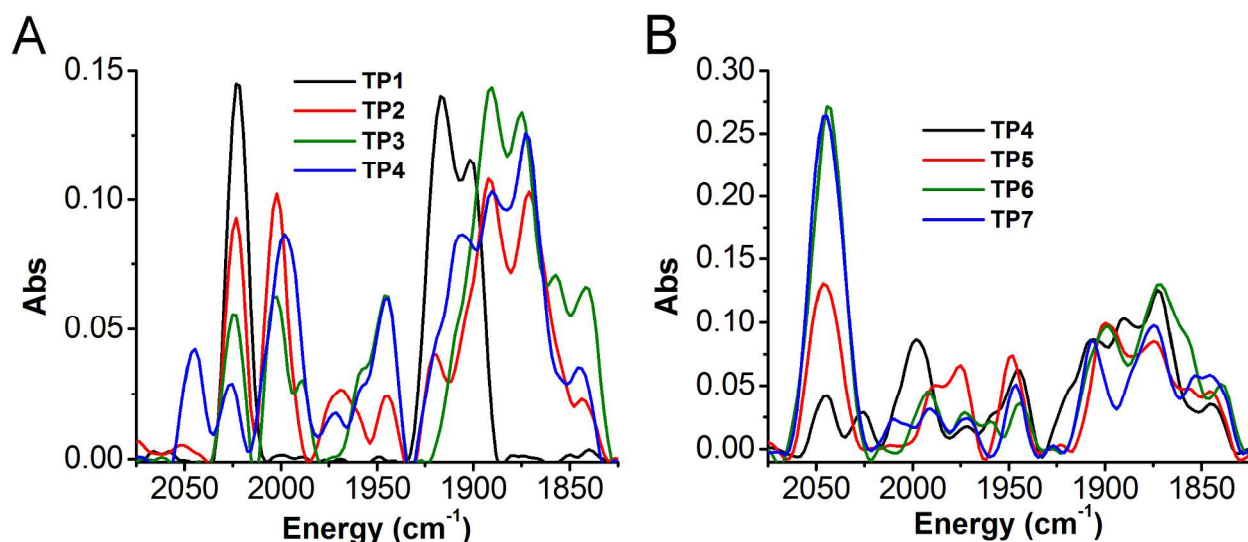


**Figure S3.** Sequentially obtained IR-SEC spectra of  $\text{Re}^{\text{I}}(\text{dmb})(\text{CO})_3\text{Cl}$  (**1B**) under conditions catalytic for the reduction of  $\text{CO}_2$  in the presence of  $\text{Ni}^{\text{II}}\text{Cp}_2$  (**14**). Growth of absorbances consistent with the formation of  $[\text{Ni}^{\text{I}}(\mu_1\text{-CO})\text{Cp}]_2$  dimer (**16**) and  $\text{Ni}(\text{CO})_4$  (**17**) are observed at  $\sim 1840\text{ cm}^{-1}$  and  $2045\text{ cm}^{-1}$ , respectively. Additional, unassigned features overlapping with Re carbonyl species are also observed between  $2000$  and  $1900\text{ cm}^{-1}$ . Reflectance IR-SEC spectra obtained in  $0.1\text{ M TBAPF}_6/\text{MeCN}$  ( $50\%\text{ CO}_2$  saturation,  $\sim 0.14\text{ M}$ ) at resting potential and  $-2.00\text{ V}$  (vs  $\text{Ag}/\text{Ag}^+$ ), respectively. Conditions:  $\text{Re}^{\text{I}}(\text{dmb})(\text{CO})_3\text{Cl}$  (**1B**,  $2.5\text{ mM}$ ),  $\text{NiCp}_2$  (**14**,  $7.8\text{ mM}$ ); glassy carbon WE, Pt CE, and Ag pseudo-RE; TP = time point.

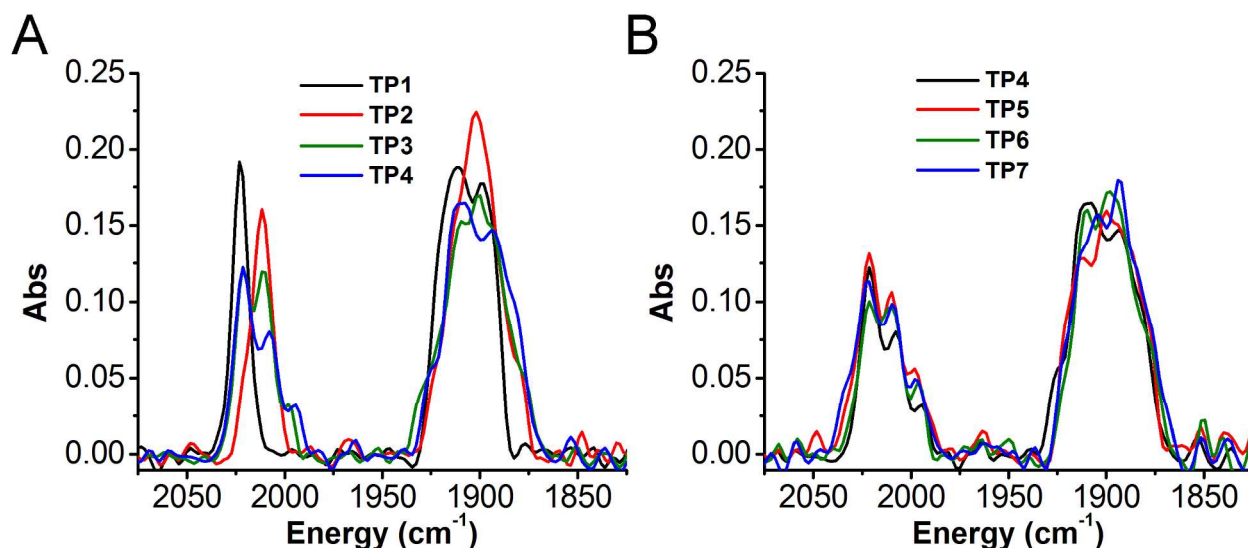


**Figure S4.** Sequentially obtained IR-SEC spectra of  $\text{Re}^{\text{I}}(\text{dmb})(\text{CO})_3\text{Cl}$  (**1B**) under conditions catalytic for the reduction of  $\text{CO}_2$ . Growth of absorbances consistent with the formation of  $[\text{Ni}^{\text{I}}(\mu_1\text{-CO})\text{Cp}]_2$  dimer (**16**) at  $\sim 1840\text{ cm}^{-1}$  and  $\text{Ni}(\text{CO})_4$  (**17**) at  $2045\text{ cm}^{-1}$  are not observed. Reflectance IR-SEC spectra obtained in  $0.1\text{ M TBAPF}_6/\text{MeCN}$  ( $50\%\text{ CO}_2$  saturation,  $\sim 0.14\text{ M}$ ) at resting potential and  $-2.00\text{ V}$  (vs  $\text{Ag}/\text{Ag}^+$ ), respectively. Conditions:  $\text{Re}^{\text{I}}(\text{dmb})(\text{CO})_3\text{Cl}$  (**1B**,  $3.5\text{ mM}$ ); glassy carbon WE, Pt CE, and Ag pseudo-RE; TP = time point.

**Table S1. Crystallographic Data for Mn<sup>I</sup>(bpy)(CO)<sub>3</sub>Br (10A)**

	Mn <sup>I</sup> (bpy)(CO) <sub>3</sub> Br (10A)
Empirical formula	C <sub>13</sub> H <sub>8</sub> BrMnN <sub>2</sub> O <sub>3</sub>
Formula weight	375.06
Temperature (K)	100(2)
Wavelength (Å)	0.71073
Space group	P $\bar{1}$ (No. 2)
<i>a</i> (Å)	10.9342(10)
<i>b</i> (Å)	11.0264(10)
<i>c</i> (Å)	11.5050(11)
<i>Alpha</i>	85.763(3)
<i>Beta</i>	85.791(3)
<i>Gamma</i>	76.792(3)
Volume (Å <sup>3</sup> )	1344.4(2)
<i>Z</i>	4
Density <sub>calcd</sub> (Mg/m <sup>3</sup> )	1.853
<i>Micro</i> (mm <sup>-1</sup> )	3.960
<i>R</i>	0.0218
<i>R<sub>w</sub></i>	0.0521

**Table S2. Crystallographic Data for [Mn<sup>0</sup>(bpy)(CO)<sub>3</sub>]<sub>2</sub> (12A)**

	[Mn <sup>0</sup> (bpy)(CO) <sub>3</sub> ] <sub>2</sub> (12A)
Empirical formula	C <sub>26</sub> H <sub>16</sub> Mn <sub>2</sub> N <sub>4</sub> O <sub>6</sub>
Formula weight	590.31
Temperature (K)	100(2)
Wavelength (Å)	0.71073
Space group	C <sub>2</sub> /c (No. 15)
<i>a</i> (Å)	9.5138(9)
<i>b</i> (Å)	19.278(2)
<i>c</i> (Å)	12.9529(11)
<i>Alpha</i>	90.00
<i>Beta</i>	104.443(4)
<i>Gamma</i>	90.00
Volume (Å <sup>3</sup> )	2300.6(4)
<i>Z</i>	4
Density <sub>calcd</sub> (Mg/m <sup>3</sup> )	1.704
<i>Micro</i> (mm <sup>-1</sup> )	1.151
<i>R</i>	0.0266
<i>R<sub>w</sub></i>	0.0628